

Synthesis, Protonation Constants, and Copper(II) and Cobalt(II) Binding Constants of a New Octaaza Macrobicyclic Cryptand: $(MX)_3(TREN)_2$. Hydroxide and Carbonate Binding of the Dicopper(II) Cryptate and Crystal Structures of the Cryptand and of the Carbonato-Bridged Dinuclear Copper(II) Cryptate[†]

Rached Menif,[‡] Joseph Reibenspies, and Arthur E. Martell*

Received May 14, 1990

A two-step synthesis in good yield of a new octaaza macrobicyclic (cryptand) ligand $(MX)_3(TREN)_2$ containing two TREN, tris(2-aminoethyl)amine, moieties bridged by three *m*-xylyl groups is reported. Protonation constants and metal ion stability constants of the mononuclear and binuclear copper(II) and cobalt(II) cryptate complexes have been measured potentiometrically and are compared with those of analogous cryptand ligands. The crystal structure of the cryptand is reported. The crystal structure of the dinuclear copper(II) cryptate is also reported and is found to be unique in the presence of a bridging carbonate ion, taken up from atmospheric CO_2 , in which the Cu(II) centers are coordinated to two different carbonate oxygens, thus forming a three-atom bridge.

Introduction

In recent years, interest in the design, synthesis, and coordination chemistry of dinucleating ligands, polydentate chelating ligands capable of simultaneously binding two metal ions in close proximity, has resulted in the study of a large number of new chelating agents.¹ Several ligand design strategies have been employed, and open-chain, macrocyclic, and macrobicyclic dinucleating ligands have been synthesized.² One of the most interesting aspects of bicyclic dinuclear complexes is their ability to further bind bridging bifunctional donor substrates, yielding "cascade" complexes.³ This paper describes the efficient synthesis of a new macrobicyclic ligand, $(MX)_3(TREN)_2$ (**1**), the determination of the crystal structure of its octahydrobromide salt, and potentiometric studies of the formation of its mono and dinuclear cryptates with Cu(II) and Co(II). Bridged cascade-type species for the dicopper(II) cryptate are found in solution with hydroxide bridging and in the solid state with carbonate bridging as demonstrated by the determination of the crystal structure of $(Cu^{2+})_2(MX)_3(TREN)_2(\mu-CO_3^{2-})(Br^-)_3 \cdot H_3O^+ \cdot 3H_2O$.

Experimental Section

Synthesis of $(MX)_3(TREN)_2 \cdot 8HBr$ (See Scheme I). A solution of 97% *m*-phthalaldehyde (2.012 g, 15 mmol) in MeCN (150 mL) was added dropwise to a stirred solution of tris(2-aminoethyl)amine (TREN) (1.50 mL, 10 mmol) in MeCN (250 mL) over 2 h at room temperature. Shiny colorless crystals formed after 12 h and were filtered out. The 200-MHz ¹³C NMR spectra in CDCl₃ gave δ (in ppm relative to TMS) 55.98 and 60.00 (CH₂ of TREN moiety); 127.36, 128.99, 132.37, and 136.87 four nonequivalent aromatic carbons; and 160.72 (CH of imine bonds). The product did not exhibit carbonyl resonance in the ¹³C NMR spectrum, which indicates that the Schiff base condensation was complete. The 200-MHz ¹³C NMR spectrum gave δ (in ppm relative to TMS) 2.6-3.8 (very broad unresolved multiplet, I = 8), 5.3 (singlet, H₂ deshielded by the imine bonds, I = 1), 7.53 (triplet, H₃ coupled to two equivalent protons H₄ and H₆), 7.59 (singlet, two equivalent protons H₇ and H₈, I = 2), and 8.2 (doublet, two equivalent protons H₄ and H₆ coupled to H₅, I = 2).

A suspension of 2.17 g of the Schiff base in 50 mL of absolute ethanol was hydrogenated with sodium borohydride. When the reaction was complete, the solvent was removed under reduced pressure, and the product was extracted with CH₂Cl₂ from aqueous solution (CH₂Cl₂/H₂O = 120 mL/10 mL). A colorless oil was obtained upon removal of the CH₂Cl₂ solvent under reduced pressure. A 5-mL aliquot of 48% HBr was added to the reduced Schiff base. A white precipitate formed and was redissolved in a H₂O/CH₃CN mixture (20 mL/200 mL). After 2 weeks at room temperature, shiny white crystals were obtained. A 200-MHz ¹³C NMR spectrum in D₂O gave δ (ppm relative to TMS)

45.90, 50.86, and 51.45 (three nonequivalent aliphatic CH₂) and 129.98, 131.17, 131.37, and 132.21 (four nonequivalent aromatic carbons). Anal. Calcd for C₃₆H₅₄N₈·8HBr: C, 34.70; H, 5.01; N, 8.99. Found: C, 34.43; H, 4.98; N, 8.91.

Potentiometric Determinations. Potentiometric p[H] measurements and computation of the protonation constants and the Cu(II) and Co(II) binding constants of the saturated octaaza cryptand $(MX)_3(TREN)_2 \cdot 8HBr$ were carried out by procedures described in detail elsewhere.⁴ The p[H] measurements were made at 25.0 ± 0.1 °C and ionic strength 0.100 M adjusted with KNO₃. Typical concentrations of experimental solutions were 0.001 00 M in ligand and 0.100 M in KOH. Typical initial solution volumes were 50.0 mL. Oxygen and carbon dioxide was excluded from the reaction mixture by maintaining a slight positive pressure of purified nitrogen in the reaction cell. Standard stock solutions of Cu(II) and Co(II) were prepared from analytical grade Cu(NO₃)₂ and Co(NO₃)₂. The pH meter-glass electrode system was calibrated to read hydrogen ion concentration directly so that the measured quantity was -log [H⁺], designated as p[H]. Log *K_w* for the system, defined in terms of log ([H⁺][OH⁻]), was found to be -13.78 at the ionic strength employed.

Preparation of the Crystalline Octahydrobromide Salt of the Hexaaza Cryptand Ligand, C₃₆H₅₄N₈·8HBr. As indicated previously in the synthesis section, during the purification of the acid form of the cryptand ligand by recrystallization from H₂O/CH₃CN (20 mL/200 mL), shiny white crystals were obtained and found to be suitable for X-ray diffraction studies.

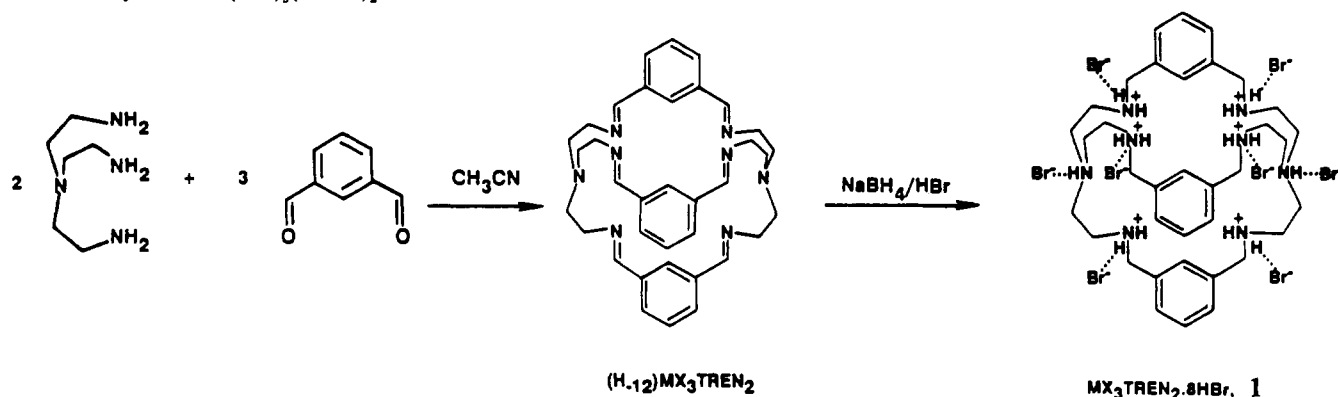
Preparation of Crystalline $[Cu_2(\mu-CO_3)(MX)_3(TREN)_2]Br_3 \cdot H_3O \cdot 3H_2O$, C₃₇H₆₃N₈O₇Cu₂Br₃. A 0.10 mmol sample of $(MX)_3(TREN)_2 \cdot 8HBr$ (124 mg) and 0.20 mmol of CuBr₂ (44.7 mg) were dissolved in 20 mL of distilled H₂O. Then 10 mL of 0.100 N KOH was added slowly to the stirred copper ligand solution. Precipitation of an amorphous green solid occurred overnight. The purpose was to prepare crystals of Cu₂(μ-OH)((MX)₃(TREN)₂)Br₃, by using the procedure reported for BIS-TREN by Motekaitis et al.⁵ To redissolve the precipitate, 1 mL of 0.100 N HNO₃ was added. The clear solution was then allowed to evaporate to the atmosphere through a small opening. Blue green crystals formed over a period of 3-4 weeks and were found to be suitable for X-ray structure determination. As indicated below, the crystal structure showed the crystals to be $[Cu_2(\mu-CO_3)((MX)_3(TREN)_2)Br_3 \cdot H_3O]$ instead of Cu₂(μ-OH)((MX)₃(TREN)₂)Br₃; the bridging carbonate originated from atmospheric CO₂.

Structure Determination of the Cryptand. A colorless plate (0.05 mm × 0.34 mm × 0.36 mm) was mounted on a glass fiber with epoxy, at room temperature. Preliminary examination and data collection were performed on a Nicolet R3m/V X-ray diffractometer (oriented graphite monochromator; Mo Kα λ = 0.71073 Å radiation). Cell parameters were calculated from the least-squares fitting of the setting angles for 25 reflections (2θ_{av} = 18.0°). ω scans for several intense reflections indicated acceptable crystal quality. Data were collected for 4.0° ≤ 2θ ≤ 45.0°.

[†] Abstracted from a dissertation submitted by R. Menif to Texas A&M University in partial fulfillment of the requirements for the degree of Doctor of Philosophy, May 1989.

[‡] Present address: N. V. Procter and Gamble Co., European Technical Center, S.A., Brussels, Belgium.

- (1) Fenton, D. E.; Caselatto, U.; Vigato, P. A.; Vidali, M. *Inorg. Chim. Acta* **1982**, *62*, 57. Borer, L.; Sinn, E. *Ibid.* **1988**, *142*, 197.
- (2) Martell, A. E. *Adv. Supramolecular Chem.* **1990**, *1*, 145.
- (3) Lehn, J. M. *Pure Appl. Chem.* **1980**, *52*, 2441; *Science* **1985**, *227*, 849.
- (4) Martell, A. E.; Motekaitis, R. J. *Determination and Use of Stability Constants*; VCH Publishers: New York, 1989.
- (5) Motekaitis, R. J.; Rudolf, R. P.; Martell, A. E.; Clearfield, A. *Inorg. Chem.* **1989**, *28*, 112.

Scheme I. Synthesis of $(MX)_3(TREN)_2$ 

Three control reflections, collected every 97 reflections, showed no significant trends. Background was measured by stationary crystal and stationary counter technique at the beginning and end of each scan for half of the total scan time.

Lorentz and polarization corrections were applied to 7108 reflections. A semiempirical⁶ absorption correction was applied (ellipsoid approximation: $\mu_{xr} = 0.10$; $T_{max} = 1.0000$, $T_{min} = 0.5916$). Reflection intensities were profiled by employing a learnt profile technique.⁷ A total of 4517 unique observed reflections ($R_{int} = 0.04$) with $|F| \geq 2.5\sigma|F|$, were used in further calculations. The structure was solved by direct methods (XS, SHELXTL-PLUS program package⁸). Full-matrix least-squares anisotropic refinement for all non-hydrogen atoms [XLS, SHELXTL-PLUS program package⁶; number of least-squares parameters = 524; quantity minimized $\sum w(f_o - f_c)^2$; $w^{-1} = \sigma^2 F + gF^2$, $g = 0.007$]⁶ yielded $R = 0.087$, $R_w = 0.077$, and $S = 1.53$ at convergence (largest $\Delta/\sigma = 0.0140$; mean $\Delta/\sigma = -0.0001$; largest positive peak in the final Fourier difference map = $0.81 \text{ e } \text{\AA}^{-3}$; largest negative peak in the Fourier difference map = $-0.81 \text{ e } \text{\AA}^{-3}$). The extinction coefficient χ [where $F^* = F_c/[1 + 0.002\chi F_c^2/\sin(2\theta)]$]^{9,10} was refined to 0.00025 (6).⁸ Hydrogen atoms were placed in idealized positions with isotropic thermal parameters fixed at 0.08. Hydrogen atoms bound to the water could not be found in the final electron density map and were omitted from the atoms list. Neutral-atom scattering factors and anomalous scattering correction terms were taken from refs 9 and 10.

Structure Determination of the Carbonato-Bridged Dinuclear Copper(II) Cryptate. A blue-green plate was mounted on a glass fiber with vacuum grease at room temperature and cooled to 193 K in a N_2 cold stream (Nicolet LT-2). Preliminary examination and data collection were performed on a Nicolet R3m/V X-ray diffractometer (oriented graphite monochromator; Mo $K\alpha$ $\lambda = 0.71073 \text{ \AA}$ radiation). Cell parameters were calculated from the least-squares fitting of the setting angles for 25 reflections ($2\theta_{av} = 21.0^\circ$). ω scans for several intense reflections indicated acceptable crystal quality. The space group was assigned as Pn .¹¹ Data were collected for $4.0^\circ \leq 2\theta \leq 50.0^\circ$ at 198 K. Scan range for the data collection was 1.20° plus $K\alpha$ separation, with a variable scan rate of $1.50\text{--}15.00^\circ \text{ min}^{-1}$. Three control reflections, collected every 97 reflections, showed no significant trends. Background measurements were made by the stationary crystal and stationary counter technique at the beginning and end of each scan for 0.50 of the total scan time.

Lorentz and polarization corrections were applied to 4230 reflections. A semiempirical⁶ absorption correction was applied (ellipsoid approximation; $\mu_{xr} = 0.05$; $T_{max} = 0.9655$, $T_{min} = 0.7509$). A total of 3604 unique reflections, with $|I| \leq 1.3\sigma|I|$, were used in further calculations.

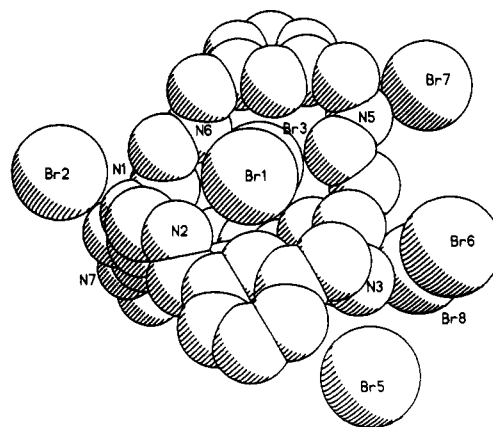


Figure 1. Space-filling diagram of the cryptand.

The structure was solved by a Patterson synthesis (XS, SHELXTL-PLUS program package⁶). Full-matrix least-squares isotropic refinement for C50, C50', O51, O51', O52, O52', O53, and O53' and anisotropic refinement of all remaining non-hydrogen atoms [XLS, SHELXTL-PLUS program package⁶; number of least-squares parameters = 507; quantity minimized $\sum w(F_o - F_c)^2$; $w^{-1} = \sigma^2 F + gF^2$, $g = 0.00010$]⁶ yielded $R = 0.055$, $R_w = 0.049$, and $S = 1.89$ at convergence (largest $\Delta/\sigma = 0.1048$; mean $\Delta/\sigma = 0.0039$; largest positive peak in the final Fourier difference map = $1.03 \text{ e } \text{\AA}^{-3}$; largest negative peak in the final Fourier difference map = $-0.90 \text{ e } \text{\AA}^{-3}$). The Rogers¹² absolute configuration parameter η was refined to 0.86 (4) and the Hamilton significance test indicated the correct absolute configuration was chosen.¹³ Hydrogen atoms were placed in idealized positions with isotropic thermal parameters fixed at 0.08. Hydrogen atoms for the hydronium ion and water molecules were located in the difference Fourier map and included in the atom list with fixed isotropic thermal parameters. Neutral-atom scattering factors and anomalous scattering correction terms were taken from refs 9 and 10.

The bridging carbonate ligand was found to be disordered between two positions. The disordered atoms were constrained for the following atom pairs by employing the DFIX instruction in XLS.⁶ The distance between the atoms in the pairs (C50', O51'; C50', O52') were constrained to 1.22 (± 0.01) \AA . The distance between the atoms in the pair (C50', O53') was constrained to 1.30 (± 0.01) \AA . The distance between atom pairs (C50', O51'; C50', O52') and (C50', O53') for the lower occupancy disordered atoms for the bicarbonate ligand were constrained to 1.22 (1) and 1.30 (1) \AA , respectively. The distances between the higher occupancy disordered atoms of the bicarbonate ligand were not constrained. The site occupation factors for the disordered atoms were allowed to refine. The site occupation for atoms C50, O51, O52, and O53 refined to 69% occupation, while that for C51', O51', O52', and O53' refined to 31% occupation. The constrained model, corrected for variable site occupation, was then allowed to refine to convergence.

The site occupation factors for the three bromine anions were allowed to refine independently. In all three cases the site occupation factor refined to a number close to 1.0. Likewise the site occupation factors

- (6) All crystallographic calculations were performed with SHELXTL-PLUS, revision 3.4, 1988 (Sheldrick, G. M., Institut für Anorganische Chemie der Universität, Tammannstrasse 4, D-3400, Göttingen, Federal Republic of Germany) supplied by Nicolet Analytical X-ray Instruments, Madison WI, on a μ VaxII minicomputer.
- (7) Diamond, R. *Acta Crystallogr.* **1969**, *A25*, 43.
- (8) Larson, R. *Acta Crystallogr.* **1967**, *A23*, 664.
- (9) *International Tables of X-Ray Crystallography*; Ibers, J. A., Hamilton, W. D., Eds.; Kynoch Press: Birmingham, England, 1974; Vol. IV, p 99.
- (10) *International Tables of X-Ray Crystallography*; Ibers, J. A., Hamilton, W. D., Eds.; Kynoch Press: Birmingham, England, 1974; Vol. IV, p 149.
- (11) The choice of the space group Pn over $P2/n$ was based on the inspection of the noncentric distribution of various classes of reflection intensities. Successful solution and refinement of the structure confirmed the choice. Attempts at solving and refining the structure in $P2/n$ failed.

- (12) Rogers, D. *Acta Crystallogr.* **1981**, *A37*, 734. Jones, P. G. *Acta Crystallogr.* **1984**, *A40*, 660.
- (13) Hamilton significance test: Hamilton, W. B. *Acta Cryst.* **1965**, *17*, 502. We employed the program HAMM written by: Daniels, L.; Falvello, L., Texas A&M University.

Table I. Atomic Coordinates ($\times 10^4$) and Equivalent Isotropic Displacement Parameters ($\text{\AA}^2 \times 10^3$) for $(MX)_3(\text{TREN})_2 \cdot 8\text{HBr} \cdot 6\text{H}_2\text{O}$

	<i>x</i>	<i>y</i>	<i>z</i>	<i>U</i> (eq) ^a
Br1	3213 (1)	4998 (1)	8699 (1)	50 (1)
Br2	8385 (1)	5509 (1)	9462 (1)	58 (1)
Br3	3436 (2)	8357 (1)	8798 (1)	72 (1)
Br4	1371 (1)	4984 (1)	6022 (1)	63 (1)
Br5	4201 (2)	1207 (2)	3860 (1)	135 (1)
Br6	2564 (1)	7378 (2)	3495 (2)	98 (1)
Br7	1083 (1)	1254 (2)	9821 (1)	81 (1)
Br8	3411 (1)	4549 (1)	4245 (1)	63 (1)
N1	-300 (7)	5935 (8)	8171 (7)	38 (5)
C1	-251 (14)	4857 (12)	7525 (11)	69 (10)
C2	45 (10)	4111 (10)	7983 (10)	45 (7)
N2	838 (9)	3402 (10)	7625 (9)	64 (7)
C3	610 (12)	2875 (13)	6631 (11)	66 (9)
C4	1418 (12)	2095 (11)	6296 (10)	48 (7)
C5	1045 (11)	1162 (12)	5575 (10)	53 (8)
C6	1759 (12)	491 (11)	5209 (10)	52 (7)
C7	2823 (12)	768 (11)	5552 (10)	45 (7)
C8	3234 (12)	1721 (13)	6262 (11)	52 (8)
C9	2518 (12)	2391 (11)	6650 (10)	49 (7)
C10	4430 (12)	2044 (12)	6628 (11)	59 (8)
N3	4886 (9)	2527 (10)	6061 (9)	62 (7)
C11	4626 (11)	3583 (11)	6186 (9)	51 (7)
C12	5191 (11)	4381 (11)	7163 (9)	43 (7)
N4	5246 (7)	5459 (9)	7184 (7)	42 (6)
C13	6065 (10)	6209 (11)	7997 (9)	46 (7)
C14	5793 (9)	6412 (10)	8928 (9)	44 (7)
N5	6675 (8)	7179 (9)	9679 (8)	48 (6)
C15	6674 (12)	7319 (13)	10654 (10)	59 (8)
C16	5790 (10)	7863 (11)	10998 (9)	39 (7)
C17	5928 (11)	8930 (11)	11438 (10)	50 (8)
C18	5127 (12)	9457 (12)	11780 (10)	56 (8)
C19	4151 (12)	8916 (12)	11640 (10)	56 (8)
C20	3977 (10)	7843 (11)	11156 (9)	40 (7)
C21	4804 (10)	7291 (11)	10846 (9)	41 (7)
C22	2876 (10)	7250 (11)	10896 (9)	47 (7)
N6	2298 (8)	7179 (9)	9979 (8)	55 (6)
C23	1212 (9)	6606 (11)	9613 (9)	47 (7)
C24	762 (10)	6570 (13)	8680 (10)	63 (9)
C25	-1046 (10)	6460 (11)	7713 (10)	45 (8)
C26	-687 (9)	6631 (11)	6952 (9)	41 (7)
C27	-1148 (10)	7566 (11)	5897 (9)	46 (7)
N7	-1365 (9)	7337 (9)	6677 (8)	53 (6)
C28	-21 (11)	8107 (12)	6145 (10)	46 (8)
C29	220 (11)	9181 (12)	6669 (10)	51 (8)
C30	1242 (12)	9680 (12)	6903 (11)	58 (8)
C31	2036 (12)	9100 (12)	6622 (11)	53 (9)
C32	1843 (10)	8051 (13)	6098 (10)	44 (8)
C33	815 (11)	7554 (12)	5874 (10)	45 (7)
C34	2740 (11)	7457 (12)	5873 (10)	52 (8)
N8	3068 (8)	6973 (9)	6553 (8)	51 (6)
C35	4149 (10)	6600 (11)	6595 (10)	48 (8)
C36	4176 (9)	5828 (10)	7023 (9)	40 (7)
O1W	3915 (9)	979 (9)	562 (8)	90 (7)
O2W	9851 (10)	8106 (9)	1847 (9)	104 (7)
O3W	1978 (10)	9274 (11)	2865 (10)	118 (9)
O4W	1659 (11)	9169 (11)	425 (13)	156 (12)
O5W	2929 (14)	1615 (12)	2199 (12)	164 (11)
O6W	320 (23)	1045 (14)	1582 (12)	285 (17)

^aEquivalent isotropic *U* defined as one-third of the trace of the orthogonalized U_{ij} tensor.

were refined independently for all three waters and the hydronium ion. In all cases the site occupation factor refined to a number close to 1.0. It was concluded that the bromines, waters, and the hydronium ion fully occupy their respective sites.

Results

Structure of $(MX)_3(\text{TREN})_2 \cdot 8\text{HBr} \cdot 6\text{H}_2\text{O}$. The structure of $(MX)_3(\text{TREN})_2$ was confirmed by crystallographic analysis of its octahydrobromide salt, in which all eight nitrogen atoms are protonated. Tables of atomic coordinates, bond lengths, and angles are given in Tables I and II, respectively. A summary of crystallographic results is given in Table III. Tables of anisotropic thermal parameters, hydrogen atom coordinates, and observed and calculated structure factors are given in the supplementary

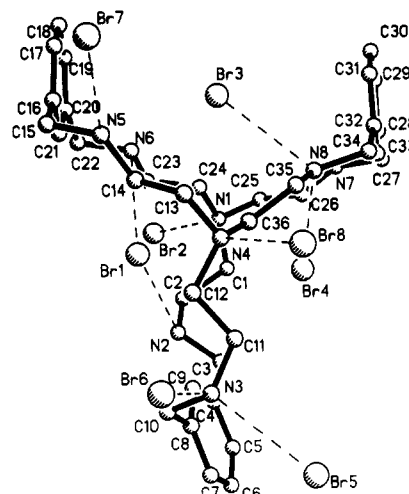


Figure 2. View of the cryptand down the axis defined by the bridgehead nitrogens, with numbering scheme.

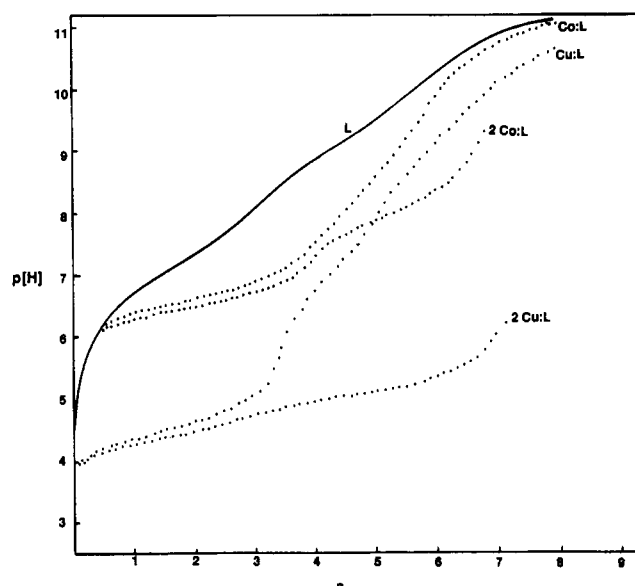


Figure 3. Potentiometric equilibrium profiles of 1.00×10^{-3} M ligand, L, in the absence of metal ion and in the presence of 1:1 and 2:1 mole ratios of Cu(II) and Co(II) to L as indicated. $\text{p[H]} = -\log [\text{H}^+]$; *a* = moles of base (0.100 M KOH) added per mole of ligand present; *t* = 25.0 °C; μ = 0.100 M, adjusted with KNO_3 .

material. Two views of the structure are shown with a space-filling diagram (Figure 1) and with a view down the axis of the bridgehead nitrogens (Figure 2). The latter shows that the cryptand is associated with three of the bromide anions, which are situated so that each one is situated on the cryptand periphery between two of the three bridges but is outside the cavity of the cryptand. The structure therefore could be described as $[3\text{Br}^-, ((MX)_3(\text{TREN})_2)(\text{H}^+)_8](\text{Br}^-)_3 \cdot 6\text{H}_2\text{O}$. The octaprotonated cryptand has a "Y" shape with the three legs being the planes of the phenyl rings (Figure 2). The length of the macrobicyclic cage (distance between the bridgehead nitrogens) is 7.60 (1) Å. The internal central cavity of the cryptand can be described as a sphere of diameter 7.4–7.6 Å. The protons located at the bridgehead nitrogens (N1 and N4) point toward the outside of the spherical internal cavity. This cavity is empty and does not contain a solvent molecule. The protonated macrobicyclic exhibits bromide anion binding (Br1, Br2, and Br4 of Figure 2), but none of the three bromide anions is located inside the internal cavity.

Protonation Constants. The potentiometric equilibrium curve of $(MX)_3(\text{TREN})_2 \cdot 8\text{HBr}$ is shown in Figure 3, and the corresponding protonation constants are given in Table IV, along with those of TREN, CBISTREN, and OBISTREN. The molecular weight determination of the acid form of the ligand by KOH

Table II. Bond Lengths (Å) and Angles (deg) for (MX)₃(TREN)₂·8HBr·6H₂O

N1-C1	1.480 (17)	N1-C24	1.487 (15)
N1-C25	1.479 (20)	C1-C2	1.520 (26)
C2-N2	1.493 (18)	N2-C3	1.436 (20)
C3-C4	1.555 (22)	C4-C5	1.356 (17)
C4-C9	1.391 (20)	C5-C6	1.389 (21)
C6-C7	1.343 (20)	C7-C8	1.375 (18)
C8-C9	1.401 (22)	C8-C10	1.511 (20)
C10-N3	1.525 (25)	N3-C11	1.480 (21)
C11-C12	1.536 (16)	C12-N4	1.505 (21)
N4-C13	1.487 (13)	N4-C36	1.493 (16)
C13-C14	1.531 (22)	C14-N5	1.497 (13)
N5-C15	1.507 (22)	C15-C16	1.474 (21)
C16-C17	1.375 (20)	C16-C21	1.400 (19)
C17-C18	1.370 (22)	C18-C19	1.373 (22)
C19-C20	1.389 (20)	C20-C21	1.399 (19)
C20-C22	1.506 (18)	C22-N6	1.472 (19)
N6-C23	1.468 (15)	C23-C24	1.475 (23)
C25-C26	1.495 (24)	C26-N7	1.477 (20)
C27-N7	1.489 (23)	C27-C28	1.511 (19)
C28-C29	1.399 (20)	C28-C33	1.391 (21)
C29-C30	1.373 (21)	C30-C31	1.366 (23)
C31-C32	1.369 (21)	C32-C33	1.380 (19)
C32-C34	1.468 (21)	C34-N8	1.502 (23)
N8-C35	1.498 (17)	C35-C36	1.495 (26)
C1-N1-C24	114.8 (11)	C1-N1-C25	111.4 (10)
C24-N1-C25	113.1 (12)	N1-C1-C2	115.1 (13)
C1-C2-N2	116.1 (15)	C2-N2-C3	114.7 (12)
N2-C3-C4	112.7 (13)	C3-C4-C5	119.0 (12)
C3-C4-C9	120.7 (11)	C5-C4-C9	119.9 (14)
C4-C5-C6	120.1 (13)	C5-C6-C7	120.4 (11)
C6-C7-C8	121.3 (14)	C7-C8-C9	118.6 (13)
C7-C8-C10	121.2 (14)	C9-C8-C10	120.2 (12)
C4-C9-C8	119.7 (11)	C8-C10-N3	111.7 (14)
C10-N3-C11	116.3 (12)	N3-C11-C12	110.6 (12)
C11-C12-N4	110.1 (12)	C12-N4-C13	112.3 (11)
C12-N4-C36	114.0 (10)	C13-N4-C36	114.8 (10)
N4-C13-C14	113.5 (11)	C13-C14-N5	107.7 (11)
C14-N5-C15	115.8 (12)	N5-C15-C16	113.6 (13)
C15-C16-C17	119.7 (13)	C15-C16-C21	119.6 (12)
C17-C16-C21	120.6 (13)	C16-C17-C18	121.0 (14)
C17-C18-C19	119.6 (14)	C18-C19-C20	120.3 (14)
C19-C20-C21	120.7 (13)	C19-C20-C22	121.0 (12)
C21-C20-C22	118.2 (12)	C16-C21-C20	117.6 (12)
C20-C22-N6	109.2 (14)	C22-N6-C23	116.2 (13)
N6-C23-C24	109.5 (14)	N1-C24-C23	116.6 (15)
N1-C25-C26	113.7 (11)	C25-C26-N7	108.8 (11)
N7-C27-C28	111.0 (11)	C26-N7-C27	116.4 (11)
C27-C28-C29	121.0 (13)	C27-C28-C33	121.2 (12)
C28-C29-C30	117.8 (13)	C28-C29-C30	121.5 (14)
C29-C30-C31	118.4 (14)	C30-C31-C32	122.5 (14)
C31-C32-C33	118.6 (14)	C31-C32-C34	120.0 (12)
C33-C32-C34	121.0 (14)	C28-C33-C32	121.1 (13)
C32-C34-N8	109.2 (14)	C34-N8-C35	115.7 (13)
N8-C35-C36	107.9 (12)	N4-C36-C35	113.6 (12)

titration gave the formula (MX)₃(TREN)₂·7.94HBr·xH₂O (5 ≤ x ≤ 6), which agrees with the crystallographic analysis finding. In solution, the bridgehead nitrogens of (MX)₃(TREN)₂ are not protonated in the p[H] range studied, 2–12. The potentiometric p[H] curve in the region a = -2 to a = 0 (where a = number of moles of OH⁻ added per mole of ligand) can be fitted by assuming neutralization of strong acid, H⁺, by strong base, OH⁻. Therefore, it is found that the bridgehead nitrogens although protonated in the solid state, as seen in the crystal structure, are not protonated even in strongly acidic solutions as low as p[H] = 2. The corresponding protonation constants are lower than 10² and cannot be measured accurately by potentiometric titration.

Metal Ion Binding and Hydroxide Bridging. The potentiometric equilibrium curves in 1:1 and 2:1 molar ratios of metal to ligand (Figure 3) with Cu(II) and Co(II) show that both mononuclear (1:1) and binuclear (2:1) complexes are formed. It is seen that the computer analysis of the data reveals the existence of a considerably larger number of species, Mono, di, and triprotonated MH_iL (i = 1, 2, 3) complexes as well as monohydroxy M_iL(OH) (i = 1, 2) species were found.

Table III. Summary of Crystallographic Results for (MX)₃(TREN)₂·8HBr·6H₂O

Crystal Data	
empirical formula	C ₃₆ H ₇₄ N ₈ O ₆ Br ₈
fw	1354.3
cryst size, mm	0.5 × 0.34 × 0.36
space group	P1 (No. 2)
unit cell dimens	
a, Å	12.838 (2)
b, Å	14.083 (3)
c, Å	16.123 (3)
α, deg	112.980 (14)
β, deg	102.030 (15)
γ, deg	91.890 (14)
vol, Å ³	2603.5 (8)
d(calcd), g/cm ³	1.728
formula units/cell	2
abs coeff, cm ⁻¹	61.49
F(000), e ⁻	1348
Data Collection	
radiation	Mo Kα (λ = 0.71073 Å)
temp, K	296
2θ range, deg	4.0–45.0
index ranges	-13 ≤ h ≤ +13, -13 ≤ k ≤ +15, -17 ≤ l ≤ 0
scan type	θ-2θ
no. of reflcns colld	7108
no. of obsd reflcns	4517 (F > 2.5σ(F))
min/max transm	0.5916/1.0000
Structure Solution and Refinement	
program package	SHELXTL PLUS (MicroVAX II)
weighting scheme	w ⁻¹ = σ ² (F) + 0.0007F ²
final residuals	R = 8.68%; R _w = 7.73%
(obsd data) ^a	
goodness-of-fit	S = 1.53

^aResiduals: $R_{\text{int}} = [\sum F^2 - (F_{\text{mean}})^2] / \sum F^2$. $R = \sum |F_o - F_c| / \sum |F_o|$. $R_w = \{[\sum w(F_o - F_c)^2] / [\sum w(F_o)^2]\}^{1/2}$. $S = \{[\sum w(F_o - F_c)^2] / [N_{\text{data}} - N_{\text{params}}]\}^{1/2}$.

Table IV. Successive Logarithmic Protonation Constants of (MX)₃(TREN)₂, OBISTREN, CBISTREN, and TREN

i	log {K _i ^H } ^a			
	(MX) ₃ (TREN) ₂ ^a	CBISTREN	OBISTREN	TREN ^b
1	9.92	10.35	9.93	10.15
2	9.26	9.88	9.31	
3	8.75	8.87	8.55	9.45
4	7.67	8.38	7.91	
5	7.16	8.14	7.32	8.43
6	6.59	7.72	6.63	

^aThis work. $\sum \text{fit} = 0.002$, average of three titrations; $t = 25.0$ °C; $\mu = 0.100$ M (KNO₃). ^bReference 20.

In the case of cobalt(II), the 1:1 and 2:1 Co:L solutions turned from a very light pinkish to green upon complexation. The 1:1 solution was clear, and the pH readings were stable even at a p[H] around 11, which is indicative of no precipitation. In the 2:1 solution again at a = 7, precipitation of a white amorphous solid occurred. The formation of a precipitate in the 2:1 systems was not reported for Cu(II) and Co(II) with BISTREN.

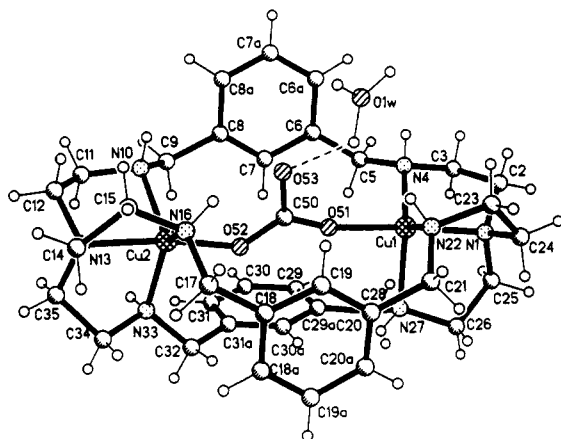
In the presence of dioxygen, the 2:1 Co:L potentiometric titration displayed a rather dark green precipitate at a = 6.5–7. The difference in the two potentiometric equilibrium curves (2:1:1 Co:L:N₂ and Co:L:O₂) is too small to compute a K_{O₂} binding constant. However, it is clear that there is oxygen interaction with the complex, since the solution turns continually darker over a period of several days. The complication of the aerobic 2:1 Co:L solution system by the appearance of a precipitate around a = 6–7, exactly where one expects the formation of the dioxygen complex, renders it very difficult to investigate the formation of a possible dioxygen cobalt adduct by potentiometric studies in solution.

Structure of [Cu(μ-CO₃)Cu(1)]Br₃. A ball and stick plot of the cation [Cu₂(μ-CO₃)(MX)₃(TREN)₂(H₂O)]³⁺ with labeling

Table V. Logarithmic Formation Constants^a of Metal Chelates of (MX)₃(TREN)₂, OBISTREN,^b and TREN^c

equilibrium quotient	log <i>K_f</i>					
	Cu(II)			Co(II)		
	(MX) ₃ (TREN) ₂ ^d	OBISTREN	TREN	(MX) ₃ (TREN) ₂	OBISTREN	TREN
[ML]/[M][L]	16.79	16.54	18.50	9.81	11.20	12.7
[M ₂ L]/[M] ² [L]	26.20	29.21		13.56	16.80	
[MLOH]/[H]/[ML]	-9.70	-10.23	-9.17	-11.01	-9.13	-9.9
[M ₂ LOH]/[H]/[M ₂ L]	-4.58	-4.26		-7.81	-7.20	
[MHL]/[ML][H]	8.65	8.78		9.10	8.53	
[MH ₂ L]/[MHL][H]	7.29	7.70		8.07	7.16	
[MH ₃ L]/[MH ₂ L][H]	6.23	6.87		6.38	6.85	

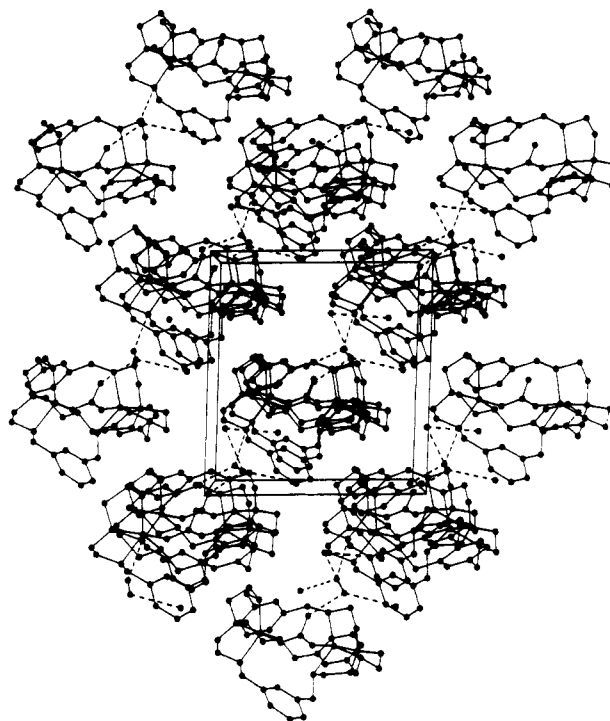
^a *t* = 25.0 °C; *μ* = 0.100 M NO₃. ^b Reference 21. ^c Reference 20. ^d This work (Σ fit = 0.01 for [1:1], 0.075 for [2:1]). ^e This work (Σ fit = 0.008 for [1:1], 0.008 for [2:1]).

**Figure 4.** Ball and stick plot of the cation [Cu₂(μ-CO₃)((MX)₃(TREN)₂)(H₃O)]³⁺ with labeling scheme.

scheme is shown in Figure 4. A packing diagram viewed along the *b* axis is shown in Figure 5. Tables of atomic coordinates and bond length and angles are given in Tables VI and VII respectively. A summary of crystallographic results is given in Table VIII. Tables of anisotropic thermal parameters, hydrogen atom coordinates, and observed and calculated structure factors are given in the supplementary materials.

The compound [Cu₂(μ-CO₃)((MX)₃(TREN)₂)(H₃O)]Br₃·3H₂O crystallized in the space group *Pn* with two cations, six bromines, two hydronium ions, and six waters per cell. The cation consists of two five-coordinate copper(II) atoms separated by 5.850 (1) Å. The copper atoms are simultaneously bridged by the binucleating ligand (MX)₃(TREN)₂ and the oxygen atoms of the exogenous ligand.

Two isoelectronic candidates (NO₃⁻ and CO₃²⁻) for the exogenous ligand were possible, based upon the synthetic pathway. Both ligands have trigonal geometry and could be isostructural. The NO₃⁻ ligand was initially assumed and the structure refined to *R_w* = 0.0586 (for 3604 reflections and 493 parameters) with the NO₃⁻ ligand refined isotropically and all remaining non-hydrogen atoms refined anisotropically. However when the NO₃⁻ ligand was allowed to refine anisotropically, the central atom went nonpositive definite. The exogenous ligand was reassigned as CO₃²⁻ and the structure was refined to an *R_w* = 0.0577 (for 3604 reflections and 493 parameters) with the CO₃²⁻ ligand refined isotropically. The differences in the weighted residuals is significant, indicating that the CO₃²⁻ model is correct.¹³ However, further anisotropic refinement indicated unusual thermal parameters for the nonbridging oxygen, the central atom, and one coordinated oxygen atom to the exogenous ligand, indicating possible disorder in the ligand. Two components of the disorder were eventually identified. The major component (69% occupation) is a CO₃²⁻ ligand. The second component may be generated by pivoting the major component 8° about a coordinated oxygen atom (O51) toward the coordinating copper atom (Cu2). The identity of the minor component could not be determined precisely and was finally assigned as CO₃²⁻ based on the near proximity of a water molecule that may serve as the hydronium ion. The resulting

**Figure 5.** Packing diagram for [Cu₂(μ-CO₃)((MX)₃(TREN)₂)(H₃O)]Br₃·3H₂O viewed along the *b* axis.

disordered atoms were included in the atom list and refined isotropically. Distances in the minor component were constrained to idealized values.

The coordination geometry about each copper(II) atom is best described as trigonal bipyramidal with the carbonate oxygen atoms and tertiary nitrogen atoms of the (MX)₃(TREN)₂ ligand occupying the axial sites and the secondary nitrogen atoms of the (MX)₃(TREN)₂ ligand occupying the equatorial sites. The cation resembles the free (MX)₃(TREN)₂ ligand in the overall "Y" shape with the uncoordinated oxygen atom of the carbonate ligand directed between two of the (MX)₃(TREN)₂ legs.

The cation is hydrogen bonded to adjacent bromine and water molecules, which in turn form a three-dimensional network of cation, bromine, and water molecules, which bisects the plane formed by the *a,c* axis of the unit cell (see Figure 5).

Discussion

Synthesis. The product obtained by condensation of m-phthalaldehyde and TREN is identified as the hexa Schiff base (MX)₃(TREN)₂. The synthesis of this compound under different experimental conditions (refluxing alcohol) was reported by McDowell and Nelson.¹⁴ The advantage of the presently used reaction conditions is a 50% higher yield; 2.17 g of macrobicyclic hexaimine was obtained, i.e. 3.7 mmol; yield 74%. (McDowell and Nelson¹⁴ reported a yield of 47–56%.) The conditions described in this research (MeCN, room temperature) represent a

(14) McDowell, D.; Nelson, J. *Tetrahedron Lett.* **1988**, *29*, 385.

Table VI. Atomic Coordinates ($\times 10^4$) and Equivalent Isotropic Displacement Parameters ($\text{\AA}^2 \times 10^3$) for $[\text{Cu}_2(\mu\text{-CO}_3)((\text{MX})_3(\text{TREN})_2)(\text{H}_2\text{O})]\text{Br}_3 \cdot 3\text{H}_2\text{O}$

	x	y	z	$U(\text{eq})^a$
Cu1	-6036 (1)	9129 (1)	3636 (1)	23 (1)
Cu2	-2631 (1)	5995 (1)	3776 (1)	19 (1)
C50	-4503 (17)	7308 (17)	3816 (17)	39 (4)
C50'	-4496 (30)	7215 (30)	4066 (27)	39 (4)
O51	-5044 (9)	8032 (9)	3518 (11)	21 (3)
O51'	-5270 (19)	7827 (18)	3944 (24)	21 (3)
O52	-3580 (10)	7039 (11)	3495 (10)	17 (2)
O52'	-3834 (23)	7024 (25)	3427 (21)	17 (2)
O53	-4833 (12)	6794 (13)	4612 (11)	41 (3)
O53'	-4611 (26)	6479 (24)	4740 (20)	41 (3)
N1	-7073 (7)	10343 (7)	3603 (7)	22 (3)
C2	-8162 (9)	9932 (9)	3434 (9)	29 (4)
C3	-8133 (9)	9055 (10)	2671 (9)	33 (4)
N4	-7305 (8)	8285 (7)	3010 (7)	26 (3)
C5	-7136 (11)	7480 (9)	2229 (9)	34 (4)
C6	-6719 (9)	6458 (9)	2639 (9)	26 (4)
C6A	-7388 (10)	5836 (10)	3187 (9)	35 (5)
C7	-5703 (10)	6086 (9)	2410 (8)	26 (4)
C7A	-7004 (10)	4884 (10)	3526 (10)	36 (5)
C8	-5346 (9)	5133 (9)	2730 (8)	24 (4)
C8A	-6005 (10)	4516 (10)	3309 (9)	32 (4)
C9	-4264 (10)	4715 (10)	2475 (9)	30 (4)
N10	-3522 (8)	4612 (7)	3309 (7)	24 (3)
C11	-2694 (10)	3835 (9)	3099 (11)	39 (5)
C12	-1862 (10)	3882 (9)	3955 (10)	32 (4)
N13	-1415 (7)	4964 (7)	4063 (7)	19 (3)
C14	-1041 (9)	5140 (9)	5078 (8)	27 (4)
C15	-2010 (10)	5424 (9)	5688 (9)	33 (4)
N16	-2518 (7)	6335 (7)	5256 (6)	20 (3)
C17	-1941 (10)	7311 (9)	5635 (9)	34 (4)
C18	-2371 (9)	8322 (9)	5205 (9)	24 (4)
C18A	-1727 (10)	8911 (10)	4605 (9)	32 (4)
C19	-3345 (9)	8740 (8)	5463 (9)	24 (4)
C19A	-2081 (11)	9876 (10)	4240 (10)	40 (5)
C20	-3714 (9)	9691 (9)	5104 (9)	25 (4)
C20A	-3100 (10)	10245 (9)	4487 (9)	32 (4)
C21	-4770 (9)	10122 (9)	5430 (9)	25 (4)
N22	-5725 (7)	9505 (7)	5093 (7)	21 (3)
C23	-6718 (9)	10060 (9)	5353 (9)	29 (4)
C24	-6988 (9)	10862 (9)	4599 (9)	28 (4)
C25	-6753 (10)	11071 (10)	2835 (9)	33 (4)
C26	-5565 (10)	11131 (9)	2756 (10)	32 (4)
N27	-5115 (7)	10065 (7)	2607 (7)	22 (3)
C28	-5135 (9)	9764 (9)	1562 (8)	26 (4)
C29A	-4442 (10)	8821 (9)	1364 (9)	29 (4)
C29	-4749 (9)	8193 (9)	525 (9)	28 (4)
C30A	-3506 (8)	8575 (9)	1846 (9)	21 (4)
C30	-4110 (10)	7348 (8)	286 (8)	25 (4)
C31A	-2852 (9)	7717 (9)	1620 (8)	23 (4)
C31	-3178 (9)	7108 (9)	829 (8)	22 (4)
C32	-1839 (9)	7536 (8)	2182 (8)	23 (4)
N33	-1691 (7)	6466 (7)	2583 (7)	24 (3)
C34	-620 (9)	6294 (9)	2979 (9)	28 (4)
C35	-547 (9)	5148 (9)	3366 (9)	26 (4)
Br1	-8909 (1)	7601 (1)	5079 (1)	42 (1)
Br2	568 (1)	6937 (1)	232 (1)	40 (1)
Br3	-10491 (1)	11748 (1)	2461 (1)	50 (1)
O1W	-6494 (7)	7029 (7)	5599 (7)	51 (3)
O2W	-3994 (12)	6238 (13)	6851 (16)	210 (11)
O3W	-6164 (11)	4846 (8)	5966 (8)	95 (5)
O4W	-13113 (7)	11272 (6)	2242 (7)	48 (3)

^a Equivalent isotropic U defined as one-third of the trace of the orthogonalized U_{ij} tensor.

valuable high-yield ($\sim 75\%$), high-quantity (> 2.0 g) route. Recently, McKee et al.¹⁵ also reported a high yield of $\sim 75\%$ for the Schiff base cryptate, but the procedure and reaction conditions were not described. The crystals of hexamine indicated the presence of several isomers and were not suitable for X-ray diffraction studies. This observation is in agreement with the ob-

servation in ^1H NMR of an unresolved broad aliphatic peak, suggesting that the isomerism is located in the aliphatic parts of the macrobicyclic ligands, probably along the imine double bonds. These observations differ from those of McKee et al.,¹⁵ who reported limited fluxionality in methylene chloride solution and reported the X-ray structure of a single conformation, which was considered to resemble the main conformation in solution.

To our knowledge, the macrobicyclic octaamine is a new compound;¹⁶ its synthesis was first reported by Menif.¹⁷ The existence of the reduced (hydrogenated) cryptand was briefly mentioned by McKee et al.,¹⁵ but up to the present time its synthesis and characterization have not been described by that or any other group.

Synthesis of analogous saturated polyaza macrocycles and macrobicycles such as BISDIEN and BISTREN have been achieved through several interesting synthetic routes. In a recent communication,¹⁸ we have reported the synthesis of $(\text{MX})_2$ -(DIEN)₂, a hexaza 24-membered saturated macrocyclic ligand by direct dipodal 2:2 condensation of benzene-1,3-dicarboxaldehyde with diethylenetriamine (followed by hydrogenation). In the present study, we report the synthesis of the analogous octaaza saturated macrobicyclic, $(\text{MX})_3(\text{TREN})_2$ (1), by direct tripodal 3:2 condensation of benzene-1,3-dicarboxaldehyde with tris(2-aminoethyl)amine (TREN). The synthesis of the saturated binucleating polyaza macrocycle and its analogous macrobicyclic via efficient and facile (amine and aldehyde) condensation (Scheme II) clearly represents a valuable route to pairs of analogous macrocyclic and macrobicyclic ligands.^{14,16,19} In view of the importance of macrocyclic and macrobicyclic ligands in the fields of molecular recognition, catalysis, and transport, the study of the effect of adding a bridge to a given macrocycle on the chemistry of the resulting cryptand should generate insights about the importance of the encapsulation of pairs of metal ions in the crypt, compared to coordinating them to the more flexible macrocyclic ligands. It is hoped that determination of crystal structures of corresponding pairs of ligands and their complexes will contribute to the understanding on the molecular level of the importance of rigidity in the stabilization of the dinuclear structures and the binding of secondary bridging bifunctional donor groups.

The protonation constants are analogous to those of OBIS-TREN. A more relevant comparison would have been with CBISTREN; however, its protonation constants have not been measured in KNO_3 , the supporting electrolyte medium used here. Indeed, Motekaitis et al.²¹ have shown that nitrate bridging does occur in the OBISTREN cryptand and results in increasing the fourth, fifth, and sixth protonation constants. Thus it is believed that the corresponding protonation constants of $(\text{MX})_3(\text{TREN})_2$ measured in NaClO_4 would be lower (for the last three) and thus the cryptand $(\text{MX})_3(\text{TREN})_2$ would have more basic amino nitrogens in the nitrate medium, as does OBISTREN. There are two possible contributing factors: the complexing of nitrate ion by the protonated nitrogens of the cryptand through hydrogen bonding and the rigidity of the $(\text{MX})_3(\text{TREN})_2$ cryptand (which is assumed to be higher than that of OBISTREN) which makes it more difficult for the polyprotonated ligand to change its conformation so as to minimize coulombic repulsion between the protonated nitrogens. The same trend may be observed in the comparison of $(\text{MX})_2(\text{DIEN})_2$ and BISDIEN.²²

(16) A similar reduced macrobicyclic octaamine derived from a different dialdehyde was reported by Lehn et al.: Jazwinski, J.; Lehn, J. M.; Lilienbaum, D.; Ziessel, R.; Guilhem, J.; Pascard, C. *J. Chem. Soc., Chem. Commun.* **1987**, 1691.

(17) Menif, R. Ph.D. Dissertation, Texas A&M University, College Station, TX, May 1989.

(18) Menif, R.; Martell, A. E. *J. Chem. Soc., Chem. Commun.* **1989**, 1521.

(19) Jazwinski, J.; Lehn, J. M.; Meric, R.; Vigneron, J. P.; Cesario, M.; Guilhem, J.; Pascard, C. *Tetrahedron Lett.* **1987**, *28*, 3489.

(20) Smith, R. M.; Martell, A. E. *Critical Stability Constants*; Plenum: New York, 1989; Vol. 6.

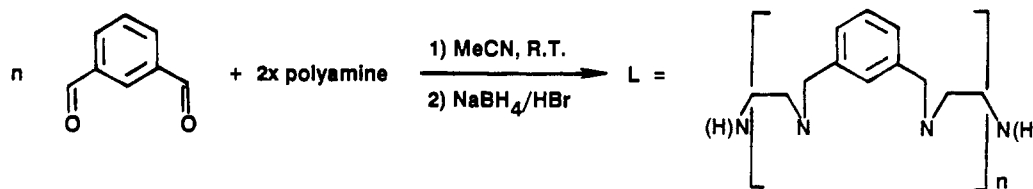
(21) Motekaitis, R. J.; Martell, A. E.; Lehn, J. M.; Watanabe, E. I. *Inorg. Chem.* **1982**, *21*, 4253.

(22) Menif, R.; Martell, A. E.; Squattrito, P.; Clearfield, A. *Inorg. Chem.* **1990**, *29*, 4723.

(15) McKee, V.; Robinson, W. T.; McDowell, D.; Nelson, J. *Tetrahedron Lett.* **1989**, *30*, 7453.

Table VII. Bond Lengths (Å) and Angles (deg) for $[\text{Cu}_2(\mu\text{-CO}_3)((\text{MX})_3(\text{TREN})_2)(\text{H}_3\text{O})]\text{Br}_3\cdot 3\text{H}_2\text{O}$

Cu1-O51	1.884 (12)	Cu1-O51'	1.960 (24)	C11-C12	1.547 (19)	C12-N13	1.498 (14)
Cu1-N1	2.024 (9)	Cu1-N4	2.083 (9)	N13-C14	1.474 (15)	N13-C35	1.491 (15)
Cu1-N22	2.084 (9)	Cu1-N27	2.207 (9)	C14-C15	1.540 (17)	C15-N16	1.446 (15)
Cu2-O52	1.821 (13)	Cu2-O52'	2.046 (30)	N16-C17	1.525 (15)	C17-C18	1.514 (16)
Cu2-N10	2.177 (9)	Cu2-N13	2.042 (9)	C18-C18A	1.392 (17)	C18-C19	1.388 (16)
Cu2-N16	2.080 (9)	Cu2-N33	2.137 (10)	C18A-C19A	1.400 (18)	C19-C20	1.387 (16)
C50-O51	1.210 (24)	C50-O52	1.297 (25)	C19A-C20A	1.412 (19)	C20-C20A	1.362 (17)
C50-O53	1.353 (27)	C50'-O51'	1.253 (44)	C20-C21	1.513 (16)	C21-N22	1.492 (14)
C50'-O52'	1.252 (47)	C50'-O53'	1.332 (48)	N22-C23	1.485 (14)	C23-C24	1.489 (17)
N1-C2	1.472 (14)	N1-C24	1.522 (15)	C25-C26	1.496 (17)	C26-N27	1.492 (14)
N1-C25	1.473 (16)	C2-C3	1.536 (17)	N27-C28	1.487 (15)	C28-C29A	1.515 (16)
C3-N4	1.492 (15)	N4-C5	1.507 (15)	C29A-C29	1.448 (17)	C29A-C30A	1.364 (16)
C5-C6	1.510 (17)	C6-C6A	1.394 (18)	C29-C30	1.390 (16)	C30A-C31A	1.409 (16)
C6-C7	1.404 (17)	C6A-C7A	1.384 (18)	C30-C31	1.398 (16)	C31A-C31	1.389 (15)
C7-C8	1.366 (16)	C7A-C8A	1.378 (17)	C31A-C32	1.481 (15)	C32-N33	1.485 (14)
C8-C8A	1.408 (17)	C8-C9	1.507 (17)	N33-C34	1.447 (14)	C34-C35	1.560 (16)
C9-N10	1.457 (15)	N10-C11	1.471 (15)				
O51-Cu1-N1	173.5 (5)	O51'-Cu1-N1	164.9 (9)	C8A-C8-C9	118.7 (10)	C7A-C8A-C8	118.9 (11)
O51-Cu1-N4	94.2 (4)	O51'-Cu1-N4	90.6 (8)	C8-C9-N10	113.8 (10)	Cu2-N10-C9	117.8 (7)
N1-Cu1-N4	84.7 (4)	O51-Cu1-N22	98.8 (5)	Cu2-N10-C11	104.4 (7)	C9-N10-C11	110.0 (9)
O51'-Cu1-N22	85.1 (10)	N1-Cu1-N22	86.8 (4)	N10-C11-C12	106.6 (10)	C11-C12-N13	110.6 (9)
N4-Cu1-N22	129.3 (4)	O51-Cu1-N27	89.4 (5)	Cu2-N13-C12	107.7 (7)	Cu2-N13-C14	107.2 (7)
O51'-Cu1-N27	109.7 (8)	N1-Cu1-N27	85.2 (3)	C12-N13-C14	110.0 (9)	Cu2-N13-C35	109.1 (7)
N4-Cu1-N27	115.0 (4)	N22-Cu1-N27	113.9 (3)	C12-N13-C35	111.1 (9)	C14-N13-C35	111.7 (9)
O52-Cu2-N10	102.0 (5)	O52'-Cu2-N10	95.0 (9)	N13-C14-C15	108.7 (9)	C14-C15-N16	108.0 (9)
O52-Cu2-N13	172.6 (5)	O52'-Cu2-N13	177.5 (9)	Cu2-N16-C15	104.3 (7)	Cu2-N16-C17	121.4 (7)
N10-Cu2-N13	84.5 (3)	O52-Cu2-N16	94.4 (5)	C15-N16-C17	108.8 (9)	N16-C17-C18	114.1 (9)
O52'-Cu2-N16	96.9 (8)	N10-Cu2-N16	118.4 (4)	C17-C18-C18A	119.2 (10)	C17-C18-C19	122.1 (10)
N13-Cu2-N16	85.4 (4)	O52-Cu2-N33	90.1 (5)	C18A-C18-C19	118.3 (10)	C18-C18A-C19A	120.4 (11)
O52'-Cu2-N33	93.3 (9)	N10-Cu2-N33	107.0 (4)	C18-C19-C20	122.1 (11)	C18A-C19A-C20A	119.1 (12)
N13-Cu2-N33	84.6 (4)	N16-Cu2-N33	132.1 (4)	C19-C20-C20A	119.3 (11)	C19-C20-C21	119.9 (10)
O51-C50-O52	125.6 (21)	O51-C50-O53	117.6 (19)	C20A-C20-C21	120.7 (10)	C19A-C20A-C20	120.6 (11)
O52-C50-O53	116.5 (18)	O51'-C50'-O52'	123.6 (36)	C20-C21-N22	114.5 (9)	Cu1-N22-C21	122.8 (7)
O51'-C50'-O53'	115.7 (34)	O52'-C50'-O53'	116.1 (35)	Cu1-N22-C23	102.1 (7)	C21-N22-C23	109.9 (8)
Cu1-O51-C50	154.6 (16)	Cu1-O51'-C50'	158.5 (25)	N22-C23-C24	109.6 (10)	N1-C24-C23	109.5 (9)
Cu2-O52-C50	134.8 (14)	Cu2-O52'-C50'	117.4 (25)	N1-C25-C26	112.3 (10)	C25-C26-N27	110.1 (9)
Cu1-N1-C2	108.6 (7)	Cu1-N1-C24	106.7 (6)	Cu1-N27-C26	101.6 (7)	Cu1-N27-C28	119.1 (6)
C2-N1-C24	109.6 (9)	Cu1-N1-C25	108.2 (7)	C26-N27-C28	112.0 (9)	N27-C28-C29A	112.9 (9)
C2-N1-C25	112.7 (9)	C24-N1-C25	110.9 (9)	C28-C29A-C29	116.5 (10)	C28-C29A-C30A	125.7 (11)
N1-C2-C3	109.0 (9)	C2-C3-N4	107.5 (9)	C29-C29A-C30A	117.4 (11)	C29A-C29-C30	118.7 (10)
Cu1-N4-C3	107.4 (7)	Cu1-N4-C5	121.7 (7)	C29A-C30A-C31A	124.6 (11)	C29-C30-C31	121.4 (10)
C3-N4-C5	109.9 (9)	N4-C5-C6	112.3 (10)	C30A-C31A-C31	116.9 (10)	C30A-C31A-C32	120.0 (10)
C5-C6-C6A	119.3 (11)	C5-C6-C7	121.0 (11)	C31-C31A-C32	123.0 (10)	C30-C31-C31A	120.9 (10)
C6A-C6-C7	119.5 (11)	C6-C6A-C7A	118.4 (12)	C31A-C32-N33	115.6 (9)	Cu2-N33-C32	118.7 (7)
C6-C7-C8	121.3 (11)	C6A-C7A-C8A	122.4 (12)	Cu2-N33-C34	101.2 (7)	C32-N33-C34	112.5 (9)
C7-C8-C8A	119.4 (11)	C7-C8-C9	121.9 (10)	N33-C34-C35	108.3 (9)	N13-C35-C34	109.4 (9)

Scheme II

polyamine = DIEN $n = 2$ $L = \text{MX}_2\text{DIEN}_2(\text{H})$

polyamine = TREN $n = 3$ $L = \text{MX}_3\text{TREN}_2$

Metal Ion Binding. The metal ion affinities and the formation of protonated metal complexes described above are similar to those reported for BISTREN (Table V). The stability constants of the mononuclear copper(II) complex of BISTREN and $(\text{MX})_3(\text{TREN})_2$ are very close; however, the dinuclear copper(II) complex of $(\text{MX})_3(\text{TREN})_2$ has lower stability (3 log units). The extremely low $\text{p}K$ of $\text{Cu}_2((\text{MX})_3(\text{TREN})_2)(\text{OH})$, 4.58, indicates that the hydroxide ion probably bridges both copper(II) ions. In the 1:1 Cu:L system, the solution turned from very light to an intense blue upon complexation as base is added, and no precipitation was observed, even at $\text{pH} \geq 11$ where $a > 8$. In the 2:1 Cu:L system, the same blue color was observed; however, a white precipitate started to form at $a = 7$. This cannot be assumed to

be $\text{Cu}(\text{OH})_2$, which is green, but must be attributed to the formation of a rather insoluble complex species $[\text{Cu}_2\text{L}(\text{OH})_m][\text{X}]_{4-m}$ ($\text{X} = \text{Br}^-$ or NO_3^-) or to more complex oligomeric chains: ... $\text{CuLCuLCuL}...$

The Carbonato-Bridged Dinuclear Complex. The identification of a hydronium ion in close proximity to the uncoordinated oxygen atom of the exogenous ligand [$\text{O}53\cdots\text{O}1\text{W} = 2.54(1) \text{ \AA}$] (see Figure 4) suggests that the carbonate model is correct. The distance between the terminal oxygen and the hydronium ion indicates a strong hydrogen bond.^{23,24} Likewise, three hydrogen

Table VIII. Summary of Crystallographic Results for $[\text{Cu}_2(\mu\text{-CO}_3)((\text{MX})_3(\text{TREN})_2)(\text{H}_3\text{O})]\cdot\text{Br}_3\cdot 3\text{H}_2\text{O}$

Crystal Data	
empirical formula	$\text{C}_{37}\text{H}_{63}\text{N}_8\text{O}_7\text{Cu}_2\text{Br}_3$
fw	1098.8
cryst size, mm	$0.08 \times 0.20 \times 0.22$
space group	Pn (No. 7)
unit cell dimens	
<i>a</i> , Å	12.516 (3)
<i>b</i> , Å	12.792 (4)
<i>c</i> , Å	13.746 (4)
β, deg	91.89 (2)
vol, Å ³	2200 (1)
<i>d</i> (calcd), g/cm ³	1.659
formula units/cell	2
abs coeff, cm ⁻¹	37.22
Data Collection	
radiation	Mo Kα ($\lambda = 0.71073$ Å)
temp, K	193
2θ range, deg	4.0–50.0
index ranges	$-14 \leq h \leq +14, 0 \leq k \leq +15, 0 \leq l \leq +16$
scan type	θ -2 θ
no. of reflns colld	4230
no. of obsd reflns	3604 ($I > 1.3\sigma(I)$)
min/max transm	0.7506/0.9655
Structure Solution and Refinement	
program package	SHELXTL PLUS (MicroVAX II)
weighting scheme	$w^{-1} = \sigma^2(F) + 0.0001F^2$
final residuals	$R = 5.46\%$; $R_w = 4.93\%$
(obsd data) ^a	
goodness-of-fit	$S = 1.89$

^a Residuals: $R = \sum |F_o - F_c| / \sum F_o$. $R_w = \{[\sum w(F_o - F_c)^2] / [\sum w(F_o)^2]\}^{1/2}$. $S = \{[\sum w(F_o - F_c)^2] / [N_{\text{data}} - N_{\text{params}}]\}^{1/2}$.

atoms were located close to the central oxygen atom of the hydronium ion, forming a rather flat pyramid similar to the structure found in $[p\text{-CH}_3\text{C}_6\text{H}_4\text{SO}_3][\text{H}_3\text{O}]$.²⁴ One of the hydrogen atoms is found close to the otherwise uncoordinated oxygen atom of the exogenous ligand. A water molecule was also found in close proximity to the minor disorder component ($[\text{O}53' \cdots \text{O}2\text{W} = 2.99$ (3) Å), which may serve as a hydronium ion. (The thermal parameters are much higher for O2W than the remaining O2W molecule possibly due to disorder in its position due to the presence of a hydronium ion or water molecule.)

Further proof is seen in the examination of the bond lengths to the central atom of the exogenous ligand suggesting the CO_3^{2-} model is correct. The bond length to the uncoordinated oxygen atom of the exogenous ligand [$\text{C}50\text{--O}53 = 1.353$ (27) Å] is significantly longer than a bond to a bridging oxygen atom [$\text{C}50\text{--O}52 = 1.210$ (24) Å]. The terminal bond length and the remaining bridging bond length [$\text{C}50\text{--O}51 = 1.297$ (25) Å] do not differ significantly. These distances are similar to those previously reported for $[\text{Rh}_2(\text{cp}^*)_4(\mu\text{-CH}_2)_2(\text{CO}_3\text{H})]\text{BF}_4$ ²⁵ and KHCO_3 .²⁶ Also, the N–O distance for nitrate would be much smaller, while the C–O distance is longer, as observed, with further lengthening due to the hydrogen bond to the adjacent hydronium ion. Further, hydrogen bonding to nitrate is weak, and the $\text{O} \cdots \text{O}$ distance in $>\text{C}\text{--O} \cdots \text{H}\text{--}\text{OH}_2$ is too short for nitrate hydrogen bonding.

The major and minor components of the disordered carbonate ligand do not symmetrically bridge the two copper atoms. As shown in Figure 4, the angle between the coordinated oxygen atom of the major component for the bridging ligand and CuL is significantly larger [$\text{C}50\text{--O}52\text{--Cu}1 = 154.1$ (16)°] than that seen for Cu2 [$\text{C}50\text{--O}52\text{--Cu}2 = 134.8$ (14)°]. The literature search for XO_3 coordinated ligands,²⁷ where (X = N or C) indicates the

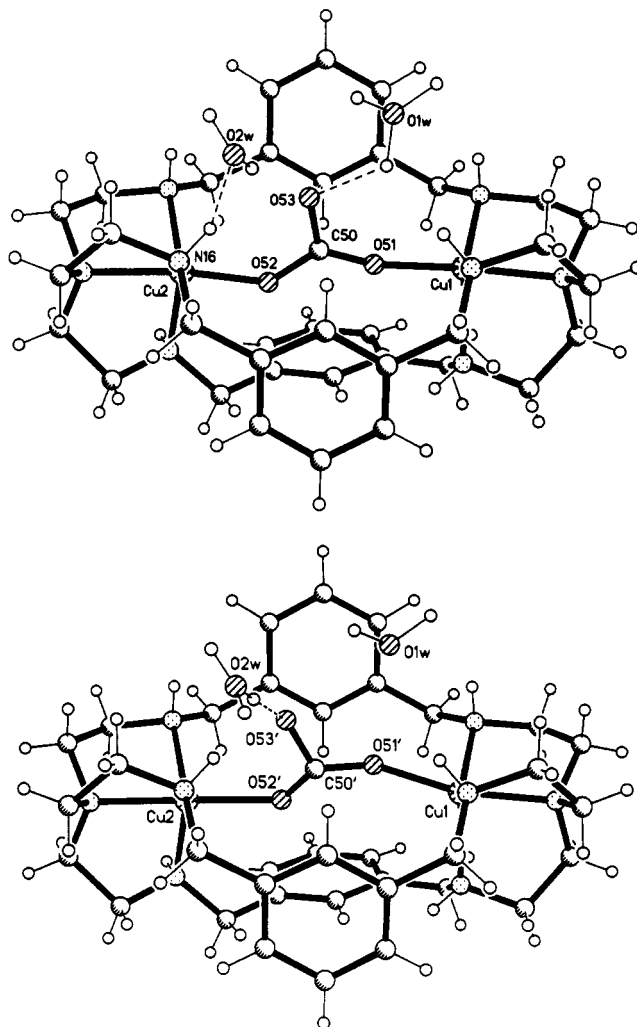


Figure 6. (a) Top: Structure of the major component of $[\text{Cu}_2(\mu\text{-CO}_3)((\text{MX})_3(\text{TREN})_2)(\text{H}_3\text{O})]\cdot\text{Br}_3\cdot 3\text{H}_2\text{O}$. (b) Bottom: Structure of the minor component of $[\text{Cu}_2(\mu\text{-CO}_3)((\text{MX})_3(\text{TREN})_2)(\text{H}_3\text{O})]\cdot\text{Br}_3\cdot 3\text{H}_2\text{O}$.

larger angle (154.1 (16)°) is unusual in XO_3 coordination.²⁸ However, such large angles are seen in complexes that have inherently restrictive steric interactions. Such a case is reported for $[\text{Ni}(\text{cyclamMe}_4)(\text{CO}_2\text{Me})_2]$,²⁹ where $\text{C--O--Ni} = 158$ and 156° and steric interactions between the methyl groups of the macrocycle prevent ideal coordination of the CO_2Me ligand.³⁰ In addition, the bond angle between the bridging oxygen atoms to the central carbon atom [$\text{O}51\text{--C}50\text{--O}52 = 125.6$ (21)°] is significantly larger than those to the uncoordinated oxygen atom [$\text{O}51\text{--C}50\text{--O}53 = 117.6^\circ$; $\text{O}52\text{--C}50\text{--O}53 = 116.5$ (18)°]. The bond lengths from the copper atoms to the coordinated oxygen atoms of the major component of the bridging ligand [$\text{Cu}1\text{--O}51 = 1.884$ (12) Å; $\text{Cu}2\text{--O}52 = 1.821$ (13) Å] do not differ considerably; however, similar bonds seen in the minor component are significantly different [$\text{Cu}1\text{--O}51' = 1.960$ (24) Å; $\text{Cu}2\text{--O}52' = 2.046$ (30) Å]. The former bond lengths are significantly shorter than those seen in similar $\mu\text{-CO}_3$ copper complexes^{31–33} and $\mu\text{-NO}_3$ copper complexes.^{34–36} This may be due, in part, to the steric

- (24) Lundgren, J.; Williams, M. J. *Chem. Phys.* **1973**, *58*, 788.
 (25) Meanwell, N. J.; Smith, A. J.; Adams, H.; Okeya, S.; Maitlis, P. M. *Organometallics* **1983**, *2*, 1705.
 (26) Thomas, J. O.; Tellgren, R.; Olovsson, I. *Acta Crystallogr.* **1974**, *B30*, 1155.
 (27) Allen, F. H.; Kennard, O.; Taylor R. *Acc. Chem. Res.* **1983**, *16*, 146.

- (28) Tyeklar, Z.; Paul, P.; Jacobson, R.; Karlin D.; Zubieta, J. *J. Am. Chem. Soc.* **1989**, *111*, 388.
 (29) Kato, M.; Ito, T. *Bull. Chem. Soc. Jpn.* **1986**, *59*, 285.
 (30) Kato, M.; Ito, T. *Inorg. Chem.* **1985**, *24*, 609.
 (31) Tyeklar, Z.; Paul, P. P.; Jacobson, R. R.; Farooq, A.; Karlin, K. D.; Zubieta, J. *J. Am. Chem. Soc.* **1989**, *111*, 338.
 (32) Gange, R. R.; Gall, R. S.; Lisensky, G. C.; Marsh, R. E.; Speltz, L. M. *Inorg. Chem.* **1982**, *18*, 771.
 (33) Churchill, M. R.; Davies, G.; El-Sayed, M. A.; Hutchinson, J. P. *Inorg. Chem.* **1982**, *21*, 1002.
 (34) Hendricks, H. M.; Birker, W. L.; van Rijn, J.; Vershoor, G. C.; Reedijk, J. *J. Am. Chem. Soc.* **1982**, *104*, 3607.
 (35) Vrabel, V.; Garaj, J. *Collect. Czech. Chem. Commun.* **1982**, *47*, 409.

crowding in the pocket of the compound and arrangement of the overall complex.

From the analysis of the crystallographic data for dinuclear copper(II) cryptate, the picture that emerges is one of a disordered carbonate bridge, with two oxygens coordinated to the Cu(II) centers. For the main component (69%) the uncoordinated carbonate oxygen is hydrogen bonded to a hydronium ion (Figure 6a), while the minor component shows the uncoordinated carbonate oxygen to be coordinated to a hydronium ion in a different position (Figure 6b). The hydronium ions are stabilized by the negative carbonate oxygens, and the water molecules involved are deprotonated (i.e. become neutral water molecules) when the carbonate oxygen is in remote positions. In other words, protonation of the water molecules to form hydrogen-bonded hydronium ions is dependent on the proximity of the negatively charged carbonate oxygen.

Finally, it should be pointed out that the Cu-O distance involving the bridging carbonate is much shorter than the Cu-O bond lengths observed for any other small anionic complexes of

that type, such as those with nitrate, carbonate, acetate, and formate, suggesting compression of the coordinate bonds to the bridging carbonate and a possible reason for the disorder. Thus the more linear arrangement of the bridging carbonate in the major component, seen in Figure 6a, while preferred, involves compression that is relieved in the minor component, Figure 6b, by distortion of the orientation of the bridging carbonate.

Acknowledgment. R.M. is indebted to L'Air Liquide, S.A., Paris, France, for financial assistance. Acknowledgment is made with thanks for support of this work by the Office of Naval Research. The R3m/V single-crystal X-ray diffraction and crystallographic computing system in the Crystal and Molecular Structures Laboratory of the Department of Chemistry, Texas A&M University, was purchased with funds provided by the National Science Foundation (Grant CHE-8513273).

Supplementary Material Available: For $(MX)_3(TREN)_2 \cdot 8HBr \cdot 6H_2O$, tables of anisotropic displacement parameters and H atom coordinates and isotropic displacement parameters and, for $Cu_2(\mu-CO_3)((MX)_3(TREN)_2)(H_2O)Br_3 \cdot 3H_2O$, tables of anisotropic displacement parameters and H atom coordinates and isotropic displacement parameters (8 pages); tables of structure factors for both compounds (40 pages). Ordering information is given on any current masthead page.

(36) Thompson, L. K.; Hanson, A. W.; Ramaswamy, B. S. *Inorg. Chem.* 1984, 23, 2459.

Contribution from the Department of Chemistry, State University of New York at Stony Brook, Stony Brook, New York 11794-3400, and Laboratoire de Chimie de Transition et de Catalyse (UA au CNRS No. 424), Institut Le Bel, Université Louis Pasteur, 4 rue Blaise Pascal, 67070 Strasbourg, France

Preparation and Structural Characterization of Dicopper(II) and Dinickel(II) Imidazolate-Bridged Macrocyclic Schiff Base Complexes

Carol A. Salata,^{1a} Marie-Thérèse Youinou,^{*1b} and Cynthia J. Burrows^{*1a}

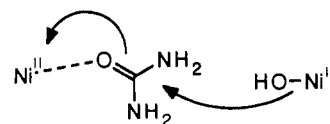
Received March 21, 1991

In order to investigate mimics of the hydrolytic enzyme urease, four new dinuclear macrocyclic complexes have been prepared by a novel template reaction, and the structure of the dicopper(II) complex with bridging imidazolate has been determined. The synthesis takes advantage of the propensity for Cu^{II} or Ni^{II} to form complexes with imidazolate. Schiff base macrocyclization of two molecules of 2,6-diacetylpyridine and two molecules of *m*-xylylenediamine occurs in the presence of 2 equiv of M^{II} and 2 equiv of ImH, leading to high yields of the dinuclear $M_2(Im)$ complexes 1-3. Systematic variation of anions and bridging ligands provided insight into the template synthesis process. For example, use of acetate in place of imidazolate as a bridging ligand led to formation of a dinickel complex, 4. A crystal structure of the copper complex $[LCu_2(\mu-Im)](CF_3SO_3)_3 \cdot H_2O \cdot 3THF$ (1) indicated a square-planar N_4 environment for each Cu with axial positions occupied by a water molecule on one Cu and two weakly bound triflates on the other Cu and showed a Cu...Cu separation of 5.92 Å. ESR and magnetic measurements of solid 1 showed antiferromagnetic coupling between the metal ions. Electrochemical studies indicated a single quasi-reversible two-electron reduction of Cu^{II} at $E_{1/2} = -435$ mV. The metal-free macrocycle was obtained by extraction of the complex with EDTA, and the $Cu_2(\mu-Im)$ group could be reintroduced by addition of 2 equiv of $Cu(CF_3SO_3)_2$ to L in the presence of ImH. Analogous dinickel(II) complexes were prepared by the same method; spectroscopic studies indicated overall similar structures. Preliminary studies of complex 4 indicate that it acts as a modest catalyst for hydrolysis of *p*-nitrophenyl acetate.

Introduction

Synthetic dinuclear transition-metal complexes provide models for metalloprotein active sites and lend insight toward the design of new catalysts. Dinuclear complexes containing copper, iron, cobalt, and zinc have been widely studied because of their relevance to dioxygen chemistry in hemocyanin, hemerythrin, superoxide dismutase, and related proteins.² In contrast, models of hydrolytic metalloenzymes have primarily focused upon mononuclear species since mononuclear Zn^{II} is the most common metal center used in enzymatic hydrolysis.³ For example, complexes of Co^{III} ,⁴ Ni^{II} ,⁵

Scheme I



Cu^{II} ,⁶ and Zn^{II} ⁷ have been shown to promote carboxylic ester and amide and phosphate ester and anhydride hydrolysis. An exception

- (1) (a) State University of New York at Stony Brook. (b) Université Louis Pasteur.
 (2) (a) Ibers, J. A.; Holm, R. H. *Science (Washington, D.C.)* 1980, 209, 223-235. (b) Que, L., Jr.; Scarrow, R. C. In *Metal Clusters in Proteins*; Que, L., Jr., Ed.; ACS Symposium Series 372; American Chemical Society: Washington, DC, 1988; pp 159-178. (c) Lippard, S. J. *Angew. Chem., Int. Ed. Engl.* 1988, 27, 344-361. (d) Tyeklár, Z.; Karlin, K. D. *Acc. Chem. Res.* 1989, 22, 241-248.
 (3) (a) Christianson, D. W.; Lipscomb, W. N. *Acc. Chem. Res.* 1989, 22, 62-69. (b) Mathews, B. W. *Acc. Chem. Res.* 1988, 21, 333-340.

- (4) For leading references, see: (a) Groves, J. T.; Baron, L. A. *J. Am. Chem. Soc.* 1989, 111, 5442-5448. (b) Chin, J.; Banaszczyk, M. *J. Am. Chem. Soc.* 1989, 111, 4103-4105. (c) Milburn, R. M.; Tafesse, F. *Inorg. Chim. Acta* 1987, 135, 119-122. (d) Schepartz, A.; Breslow, R. *J. Am. Chem. Soc.* 1987, 109, 1814-1826. (e) Hendry, P.; Sargeson, A. M. *J. Am. Chem. Soc.* 1989, 111, 2521-2527. (f) Fife, T. H.; Pujari, M. P. *J. Am. Chem. Soc.* 1988, 110, 7790-7797.
 (5) (a) Groves, J. T.; Chambers, R. R. *J. Am. Chem. Soc.* 1984, 106, 630-638. (b) Blakely, R. L.; Treston, A.; Andrews, R. K.; Zerner, B. *J. Am. Chem. Soc.* 1982, 104, 612-614. (c) De Roach, M. A.; Troglor, W. C. *Inorg. Chem.* 1990, 29, 2409-2416.